PVP-Vol. 489, Problems Involving Thermal-Hydraulics,
Liquid Sloshing, and Extreme Loads on Structures
July 25–29, 2004, San Diego, California USA
PVP2004-3048

FINITE ELEMENT MODELING OF BRINELL AND ROCKWELL HARDNESS TESTING OF METALS

William Keith Rule
SUNY Oswego, Depts. of Mathematics and Physics
218 Snygg Hall, Oswego, NY 13126, USA
(315)312-5751, wrule@oswego.edu

ABSTRACT

Hardness test results provide a convenient and economical means of specifying material performance characteristics and are useful in quality control. Quantifiable hardness testing is at least 150 years old but, due to the complex deformation processes that occur during indentation, in many ways physical insights on the test are still lacking. Finite element codes can now accurately simulate complex, time-varying stress and strain states. Such codes can be used as a tool to study the hardness test and with the knowledge gained perhaps make such testing more useful for validating the material models used for impact simulations. In this paper the EPIC finite element code with the Johnson-Cook strength model was used to numerically simulate Brinell, and Rockwell B, C, and F hardness tests (as appropriate) for 24 different metals.

INTRODUCTION

Material hardness values are often cited in manufacturing specifications and are used for quality control purposes. Hardness tests are usually convenient and economical to conduct and can often be classified as nondestructive. However, despite the fact that various types of hardness testing have been quantitatively conducted for over 150 years, a fundamental, theoretical understanding of the test is, in many aspects, still lacking. This is because the physical processes that occur during a hardness test are very complex although such tests are relatively easy to conduct. Contemporary computational mechanics techniques and computer hardware have made it possible and practical to numerically model hardness tests. The goal of such modeling is to obtain more information from the testing and thereby make the results more useful for validating the material models used for impact simulations. Numerically modeling Brinell and Rockwell hardness testing of metals is the topic of this paper.

For many years researchers have attempted to model hardness tests or similar indentation events with finite element codes. Hardy et al. (1971) first modeled the indentation of an elastic-perfectly plastic half-space by a rigid sphere. Their calculations produced good agreement with some measured contact area data obtained from the literature. Lee et al. (1972) numerically modeled an experiment where a 10 mm diameter ball was forced into a 4340 steel test piece by a screw driven testing machine. This experiment was similar to the Brinell hardness test. Their calculated results agreed reasonably well with experimentally measured loads and indenter displacements, however no attempt was made to validate a numerically estimated Brinell hardness number.

Follansbee and Sinclair (1984) numerically modeled the indentation of an elasto-plastic half-space by a rigid sphere. To validate their numerical results, a modified Rockwell hardness tester was used to slowly force (at 147, 294, 441 N) a 1.59 mm (1/16 in.) diameter high-strength tool steel indenter into flat 304L stainless steel test pieces. Their numerical results agreed well with those measured. They modeled both lubricated and adhesive contact and found little difference in the results. This provides some justification for the commonly used assumption of frictionless contact. Follansbee and Sinclair did not endeavor to simulate a standard Rockwell test however.

In 1988, Bhattacharya and Nix numerically simulated microhardness testing of nickel, silicon, and aluminum specimens. These researchers also found that modeling the effects of contact friction was not required. They were able to adequately reproduce experimentally measured load versus displacement plots for the nickel and silicon specimens. Microhardness values were calculated from the finite element results of the aluminum and silicon specimens but these results were not compared with those obtained from a standard microhardness testing device. Komvopoulos (1989), and Laursen and Simo (1992) conducted finite element simulations of the indentation of layered materials in order to study the evolution of the plastic zones beneath the indenter.

The study described in this paper was motivated by a numerical study of microhardness testing of oxygen free high conductivity (OFHC) copper using the EPIC finite element code (Chen et al., 1994). Four different indenter shapes were modeled (trigonal, Vickers, spherical, flat-ended) and calculated load versus penetration depth plots were compared with those measured. They then discussed a scheme to adjust strength model parameters in order to obtain a better fit between measured and calculated results.

In this paper, the EPIC code has been applied to simulating standard Brinell and Rockwell macrohardness tests of 24 metals. The author is not aware of previously published results of numerical simulations of these standard hardness tests.

THE EPIC FINITE ELEMENT CODE

The EPIC code was first developed some time ago by Johnson (1978) and its enhancement continues (Johnson et al., 1996). A good description of the basic numerical modeling approach used by EPIC was published by Johnson (1993). EPIC is designed to facilitate modeling the time history of impact events. Hardness testing is a type of impact event, although loading times for most hardness tests (of the order of 1 s) are typically much longer than that of a typical EPIC application (of the order of 0.1 ms). However, except for the time frame discrepancy, EPIC is ideally suited for the detailed modeling the macrohardness testing procedures commonly used in engineering practice today.

EPIC is an explicit finite element code, where, as the solution proceeds through time, new nodal positions and velocities are calculated from current nodal positions, velocities, and accelerations. An advantage of the explicit approach is that no computationally expensive matrix inversions are required - the equations of motion can be integrated directly. The explicit approach also makes treating erosion (material removal) and fragmentation relatively straight forward since the issues associated with a singular stiffness matrix do not come into play.

However, explicit methods have the disadvantage of requiring a relatively small time step size to preserve numerical stability. The time step size must be continuously adjusted as the simulation proceeds to ensure that an elastic stress wave will not be capable of passing through any element in a single time step. During impact events time steps can become quite small as elements become squashed flat. Time step sizes are often restricted to be on the order of a nanosecond. With time steps of this size it is practically impossible to run macrohardness simulations for several seconds of elapsed time.

Accordingly, some modifications were made to the modeled system to allow reasonably realistic macrohardness testing simulations to be made for accelerated simulations involving elapsed times of less than 1 ms. The first set of modifications involved the Johnson-Cook strength model (Johnson, 1993):

$$\sigma = \left(C_1 + C_2\varepsilon^n\right)\left(1 + C_3 \ln \dot{\varepsilon}^*\right)\left(1 - T^{*m}\right) \qquad (1)$$

where: σ is the yield strength (plastic flow stress); C_1, C_2, C_3, n, and m are empirical coefficients; ε is the effective plastic strain; $\dot{\varepsilon}^*$ is the normalized effective plastic strain rate; and T^* is the homologous temperature. As described by Johnson (1993) strength models play a key role in treating the plastic flow of the penetrator and target in an impact event. The strength model defines the scalar stress level (in a von Mises sense) at which plastic flow will begin in the material. In an actual macrohardness test strain rates are relatively low and so no strain rate induced increase in the yield stress is observed. To preserve this behavior in the accelerated simulation the strain rate sensitivity coefficient C_3 in equation 1 was set to zero. This modification was also made by Chen et al. (1994) in their EPIC microhardness test simulations.

Also, in actual macrohardness testing the heat generated by the plastic deformation of the test piece has sufficient time to be conducted away and so temperature increases are not significant. To maintain this condition in the accelerated testing simulation the temperature sensitive factor of equation 1 was disabled.

The accelerated simulation requires that the indenter be loaded quite rapidly. This produces two undesirable effects. On initial loading, the indenter can be failed by its own inertia reacting against the applied loading. Also, the indenter can gain a significant amount of momentum while being loaded to the peak load required for the macrohardness test being simulated. Dissipation of this momentum can result in the indenter applying a higher load than intended. To negate these negative effects the density of the indenter (based on S-7 tool steel) was reduced by a factor of ten. Larger reductions in density were attempted but this tended to interfere with the sliding interface EPIC set up between the indenter and the test piece. The sliding interface prevents the indenter and test piece from intermingling. Very low density indenters (relative to the test piece) tend to pass right through the sliding interface. However, a factor of 10 reduction in indenter density appeared to be adequate for adjusting the indenter inertia to an appropriate level.

Also, although this is not related to loading rate effects, the indenter (based on S-7 tool steel for all simulations) was made artificially stronger by factor of four to avoid plastic deformation during the test simulation. This strengthening did not affect the elastic behavior of the indenter however.

These modifications allowed accelerated simulation times of 400 μs and 620 μs for the Brinell and Rockwell hardness tests, respectively. Simulation times of these durations effectively converged. In other words, simulations of longer duration produced no significant change in the calculated results for the mesh density used. The load (normalized to unity) versus time profiles used in simulating the Brinell and Rockwell C hardness tests are shown in Fig. 1. The Rockwell B and F loading profiles were similar to that shown for Rockwell C except that relative level of the minor load was different.

Three node, triangular, axisymmetric elements were used. This type of element is commonly used in impact simulations because it is relatively insensitive to distortions and is computationally efficient. A series of runs were made with increasing mesh densities (and thus smaller elements) until the calculated hardnesses converged.

The spherical indenters (Brinell, Rockwell B, and Rockwell F hardness tests) were modeled as a hemispherical indenter connected to cylindrical component of length and radius equal to that of the spherical indenter (see Fig. 2). This was done to avoid the stress concentrations associated with point loading a spherical object. The indenter of Rockwell C hardness test was modeled with a simple, unrounded, 120° cone. The cone was also connected to a cylindrical component like that described above. Because the triangular elements used in the modeling are essentially constant strain (strains are averaged over the element), slightly rounding the indenter (as is the case in the actual test) is not required to remove the stress concentration of the "sharp" cone modeled. All numerically modeled indenters were loaded by applying a uniform pressure of an appropriate magnitude in a time varying fashion to the circular free surface of the cylindrical component of the indenter.

Most indentation simulations reported in the literature assume frictional forces between the indenter and tested materials are negligible. Frictionless contact was assumed in this study. However, EPIC has the capability for modeling friction on contact surfaces. Also, a flat, frictionless surface was placed under the test piece model for support during the simulation.

EPIC and similar codes are sophisticated analysis tools. Developing an understanding of the fine details of these codes is time consuming and generally requires specialized personnel. This has inhibited the use of advanced analysis tools in many industrial settings. However, the hardness test simulator discussed in this paper was packaged in a special purpose Microsoft Windows-based program that automatically generated the input file required by EPIC, launched EPIC, and post-processed the EPIC results. Thus, there is no need to be a computational mechanics expert to run hardness test simulations.

MODELING THE BRINELL HARDNESS TEST

The most common form of Brinell hardness testing involves producing an indentation in the test piece by applying a 3000 kg load to a hardened 10 mm diameter ball. The Brinell hardness number (HB) can be determined from measuring the indentation diameter or indentation depth. The large indentations typically produced during Brinell hardness testing have the advantage of averaging out the effects of variations in the surface roughness and the microstructure of the test piece. However, the large indentations can act as an undesirable stress concentration in the test piece.

In numerical simulations, the indentation depth can be easily determined by tracking the displacement of the test piece node directly under the tip of the indenter. This allows the Brinell hardness number to be determined from the following equation (Fee et al., 1985a):

$$HB = \frac{P}{\pi D d} \qquad (2)$$

where: P is the applied load (3000 kg), D is the indenter diameter (10 mm), and d is the depth of penetration (in mm).

For HB readings to be valid, the test piece must be sufficiently large so that edge effects do not influence the plastic flow produced by the indenter. It was recommended (Fee et al., 1985a) that the depth of the test piece be at least ten times the indentation depth, and that the indentation be at least three indentation diameters from the edge of the test piece. For this study, the test piece depth and width was set at three times the indenter radius. These dimensions appeared to be sufficiently large to numerically isolate the test piece boundaries from the indented region.

The finite element mesh used in the Brinell hardness test simulations and the final deformed geometry for the 6061-T6 aluminum test case are shown in Fig. 2. Note that a graded mesh was used, with the smallest (and therefore most accurate) test piece elements being placed in the vicinity of the indentation. A plot of applied load versus indentation depth for the Brinell hardness test simulation of 6061-T6 aluminum is shown in Fig. 3(a). Note that the loading curve of Fig. 3(a) displayed a series of jumps which are not usually observed (see Fig. 3 of Bhattacharya and Nix, 1988) in actual hardness testing. This discrepancy is probably due to the fact that the numerical calculations were accelerated to obtain practical solution times. However, convergence studies showed that sufficiently long run times were used to obtain reliable hardness predictions.

MODELING THE ROCKWELL B AND F HARDNESS TESTS

Rockwell B and F hardness tests are quite similar to the Brinell hardness test. However, these Rockwell tests use a much smaller spherical indenter (1.588 mm diameter) and smaller major loads (100 kg Rockwell B, 60 kg Rockwell F) than the Brinell hardness test. Thus, Rockwell test indentations are much smaller than those produced by the Brinell test. For most applications Rockwell hardness testing can be considered nondestructive.

Also, the loading history and method of Rockwell hardness calculation are different from those of the Brinell test (see Fig. 1). In Rockwell testing, first a minor load of 10 kg is applied to the indenter and the initial indentation, d_i, noted. Then more loading is added until the major load is applied. The additional loading is finally removed leaving the minor load applied and the final indentation, d_f, is noted. The initial and final indentations as calculated by EPIC were easily obtained by tracking the displacement of the test piece node directly under the tip of the indenter. Once these indentations are known the Rockwell B or Rockwell F hardness numbers can be determined from the following equation (Fee et al., 1985b):

$$\text{HRB or HRF} = 130 - 500(d_f - d_i) \qquad (3)$$

Note that d_i and d_f should be expressed in units of millimeters for use in equation 3. In Rockwell hardness testing, the initial indentation depth, d_i, is the baseline or datum for the hardness calculation. This approach tends to factor out test piece surface roughness variations from the final calculated hardness number.

Figure 3(b) shows a force versus indenter displacement plot generated by EPIC during a Rockwell B hardness test simulation of 6061-T6 aluminum. The horizontal lines represent minor and major load levels applied to the indenter. Note that the loading curve is characterized by a series of jumps similar to those observed in the Brinell test (Fig. 3(a)).

MODELING THE ROCKWELL C HARDNESS TEST

The Rockwell C hardness tests simulations were virtually identical to the Rockwell B and F tests described above except that hemispherical indentation surface was replaced with a 120° cone, the major load was set at 150 kg, and the hardness number was determined as follows (Fee et al., 1985b):

$$HRC = 100 - 500(d_f - d_i) \qquad (4)$$

A typical Rockwell C hardness test simulation is shown in Fig. 4.

CALCULATED HARDNESSES FOR 24 METALS

Hardness tests of twenty four metals of industrial significance where simulated with EPIC. Most of these metals cannot be identified or described in detail because of proprietary considerations.

However, three of the more commonly known metals (6061-T6 Al, 4340 Steel, OFHC Copper) will be considered in more detail. The Brinell hardness test was simulated for all the metals. In addition, the appropriate Rockwell hardness test (F - softest metals, B - medium hardness metals, C - hardest metals) was also simulated for each material. Thus, 48 hardnesses were determined altogether.

Figure 5 shows a plot of calculated Rockwell hardness (CH) versus measured Rockwell hardness (MH) for the 24 metals considered. As can be seen from this plot, EPIC tended to over-estimate the Rockwell hardness. A perfect fit would follow the dotted diagonal line of Fig. 5. This discrepancy could be partially due to the numerical difficulties associated with forcing conventional finite elements to flow around a penetrator. Such artificial resistance to flow often makes the indented material appear to be stronger or harder than it actually is. One would expect this error to increase with increasing deformation. Thus, the error associated with the softer materials should be higher. This agrees with the error pattern shown in Fig. 5.

To establish the sensitivity of the calculated hardnesses to the material properties input to the numerical model, the following study was undertaken. Three metals (6061-T6 Al, 4340 Steel, OFHC Copper), one from each Rockwell hardness test type, with large calculated hardness errors, were selected for further investigation. The measured hardness, calculated hardness and nominal material constants of these three metals are given in the top part of Table 1. The three active constants of the strength model (C_1, C_2, and n of equation 1) of each metal were then adjusted by the same factor (the simplest scheme) to obtain a calculated hardness the same as that measured. These adjusted material constants of each metal are given in the bottom portion of Table 1. The nominal and adjusted stress-strain curves (plotted according to the data of Table 1) are compared in Fig. 6. It is evident from this figure that only relatively minor changes to the strength model parameters of the 6061-T6 Al and OFHC Cu were required to produce an accurate Rockwell hardness prediction. However, Fig. 6 shows that a considerable change in the strength model parameters of the 4340 steel was required to produce an accurate Rockwell C hardness prediction.

RELATION OF CALCULATED HARDNESS TO OFFSET YIELD STRESS

Conducting a hardness test is generally more convenient and economical than performing a tension test. Accordingly, there has been an interest in estimating tension test results such as the ultimate tensile strength from hardness test data (Dieter, 1986). In this study, the relationship between 0.2 % offset yield stress (OYS) and calculated Rockwell hardness was investigated. The OYS was determined for each metal by applying equation 1 as follows:

$$OYS = C_1 + C_2 (0.002)^n \quad (5)$$

The OYS values as determined by equation 5 are plotted versus calculated Rockwell B, C, and F hardness values in Fig. 7. Least square fit lines for the three sets of Rockwell hardness data are also shown in Fig. 7.

Figure 7 shows that the OYS appears to vary linearly with Rockwell hardness number. It is important to note that the data shown in Fig. 7 is for a very wide variety of metals.

COMPARISON OF CALCULATED HARDNESS TEST CONVERSION RESULTS WITH TABULATED VALUES

It is often useful to convert from one hardness scale to another. Conversion tables have been published for this purpose. However, such references state (Lysaght and DeBellis, 1969; Fee et al., 1985c) that universal conversion tables are not available and that the conversion factors published are approximate and only valid for a certain class of materials. However, conversion factors can be conveniently calculated with a code like EPIC by simply simulating the two hardness tests of interest, and then using the appropriate ratio of the results to provide the conversion factor for the known (measured) hardness value.

As shown in Fig. 8, the relationship between the Brinell and Rockwell hardness scales was numerically investigated using EPIC. The calculations showed an approximately linear relationship between the Brinell and Rockwell B, C, and F scales. Least squares formulas for the best-fit lines are shown on Fig. 8. It is important to note that the results shown in Fig. 8 are for a very wide variety of metals. Also shown on Fig. 8 are conversion table data points for steel (Lysaght and DeBellis, 1969; Fee et al., 1985c). It is interesting that the conversion table values are approximately linear as well, with slopes close to those obtained by EPIC. However, the tabulated values are significantly offset from the best fit lines obtained from the EPIC calculations.

NON-STANDARD HARDNESS TEST GEOMETRIES

To obtain consistent hardness readings, care must be taken to ensure that specimen boundaries do not influence the plastic deformation process in the vicinity of the indentation. However, for certain test pieces (such as actual as manufactured hardware components) this may be inconvenient or impossible. It may be feasible to use a code like EPIC to calculate a conversion factor to relate the results of a non-standard hardness test to that of a standard test. For instance, a very thin or a very narrow specimen could be hardness tested and then a similar material of the same geometry numerically modeled as shown in Figures 9 and 10, respectively. A conventional hardness test could then be modeled and a conversion factor obtained by dividing this hardness value by that numerically obtained earlier for the non-standard geometry. This test geometry conversion factor could then be applied to the measured hardness value to obtain an approximation for the measured conventional hardness value. Similar geometry conversion factors could also be numerically obtained for curved surfaces.

SUMMARY

The EPIC finite element code was used to numerically simulate Brinell, and Rockwell B, C, and F hardness tests (as appropriate) for 24 different metals currently in use by various industries. Strain rate and temperature effects were removed from the material strength models, and the inertia of the indentor was reduced, to allow for practical solution times. The yield strength of the indentor (based on

S-7 tool steel) was increased by a factor of four to avoid significant plastic deformation during the simulation.

Predicted Rockwell hardness values generally exceeded those measured. However, it was found that accurate hardness predictions could be made for 6061-T6 aluminum and OFHC copper with only minor adjustments made to the input stress-strain curves. Offset yield stress was found to be a linear function of Rockwell hardness. Linear conversion functions between calculated Rockwell and calculated Brinell hardness values were obtained and compared with tabulated values from the literature. A means to numerically obtain a geometrical hardness conversion factor to allow hardness testing of non-standard geometries was discussed.

ACKNOWLEDGMENT

Professor Richard C. Bradt inspired this project by once asking if EPIC could be used to simulate standard hardness tests. For this and for many enlightening technical and other discussions over many years the author is deeply grateful.

REFERENCES

Bhattacharya, A. K., and Nix, W. D., 1988, "Finite Element Simulation of Indentation Experiments," *Int. J. Solids Structures*, Vol. 24, No. 9, pp. 881-891.

Chen, Y-M., Ruff, A. W., and Dally, J. W., 1994, "A Hybrid Method for Determining Material Properties from Instrumented Micro-Indentation Experiments," *J. Mater. Res.*, Vol. 9, No. 5, pp. 1314-1321.

Dieter, G. E., 1986, "Mechanical Metallurgy," Third Edition, McGraw-Hill Book Company, New York, p. 331.

Fee, A. R., Segabache, R., and Tobolski, E. L., 1985a, "Brinell Hardness Testing," in Metals Handbook Ninth Edition, Vol. 8 Mechanical Testing, John R. Newby Coordinator, American Society for Metals, Metals Park, Ohio, pp. 84-89.

Fee, A. R., Segabache, R., and Tobolski, E. L., 1985b, "Rockwell Hardness Testing," in Metals Handbook Ninth Edition, Vol. 8 Mechanical Testing, John R. Newby Coordinator, American Society for Metals, Metals Park, Ohio, pp. 74-83.

Fee, A. R., Segabache, R., and Tobolski, E. L., 1985c, "Appendix: Hardness Conversion Tables," in Metals Handbook Ninth Edition, Vol. 8 Mechanical Testing, John R. Newby Coordinator, American Society for Metals, Metals Park, Ohio, pp. 109-113.

Follansbee, P. S., and Sinclair, G. B., 1984, "Quasi-Static Indentation of an Elasto-Plastic Half-Space by a Rigid Sphere - I," *Int. J. Solids Structures*, Vol. 20, No. 1, pp. 81-91.

Hardy, C., Baronet, C. N., and Tordion, G. V., 1971, "The Elasto-Plastic Indentation of a Half-Space by a Rigid Sphere," *Int. J. For Num. Meth. in Eng.*, Vol. 3, pp. 451-462.

Johnson, G. R., 1978, "A Computer Program for Elastic-plastic Impact Computations in 2 Dimensions Plus Spin," Contract Report ARBRL-CR-00373, Honeywell Inc., Hopkins, Minnesota.

Johnson, G. R., 1993, "Material Characterization for Warhead Computations," in Tactical Missile Warheads, J. Carleone Editor, Vol. 155, AIAA Progress in Astronautics and Aeronautics, pp. 165-197.

Johnson, G. R., Stryk, R. A., Holmquist, T. J., and Beissel, S. R., 1996, "User Instructions for the 1996 Version of the EPIC Code," Alliant Tecksystems Inc., Hopkins, Minnesota.

Komvopoulos, K., 1989, Elastic-Plastic Finite Element Analysis of Indented Layered Media," *J.* of *Tribology*, Vol. 111, pp. 430-439.

Laursen, T. A., and Simo, J. C., 1992, "A Study of the Mechanics of Microindentation Using Finite Elements," *J. Mater. Res.*, Vol. 7, No. 3, pp 618-626.

Lee, C. H., Masaki, S., and Kobayashi, S., 1972, "Analysis of Ball Indentation," *Int. J. Mech. Sci.*, Vol. 14, pp. 417-426.

Lysaght, V. E., and DeBellis, A., 1969, "Hardness Testing Handbook," American Chain and Cable Co., Inc., pp. 136-138.

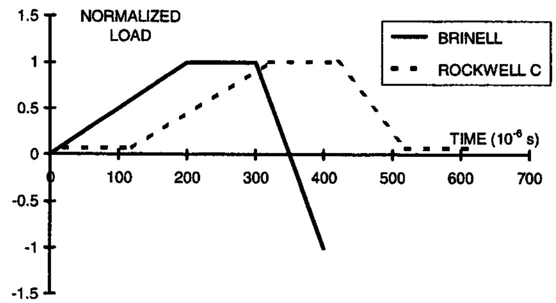

Figure 1. Normalized load versus time profiles used in numerical simulations.

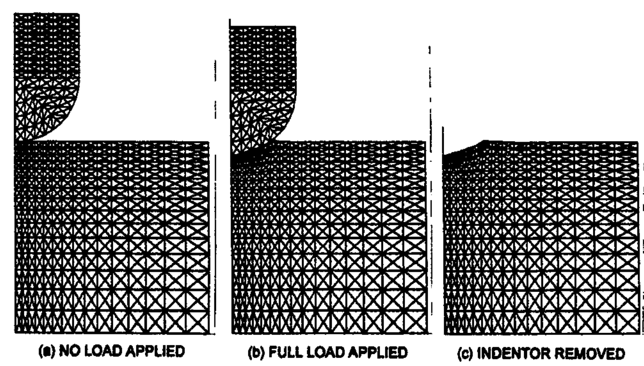

Figure 2. Finite element mesh used for Brinell hardness test simulations.

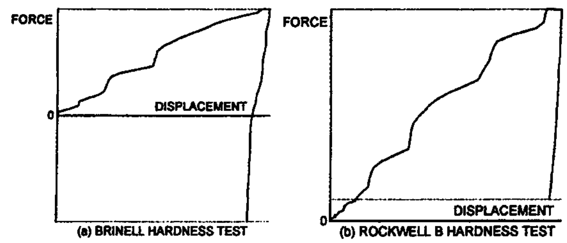

Figure 3. Force versus indenter displacement plots determined from EPIC results of hardness testing of 6061-T6 aluminum.

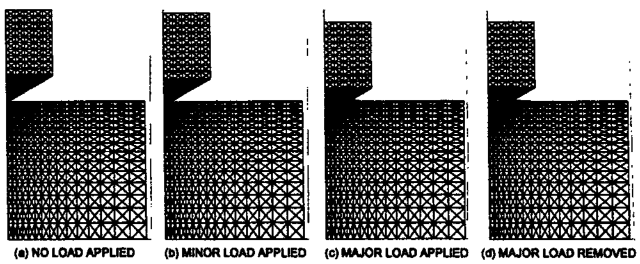

Figure 4. Typical Rockwell C hardness test simulation. Note that in (d) the minor load (10 kg) is still applied.

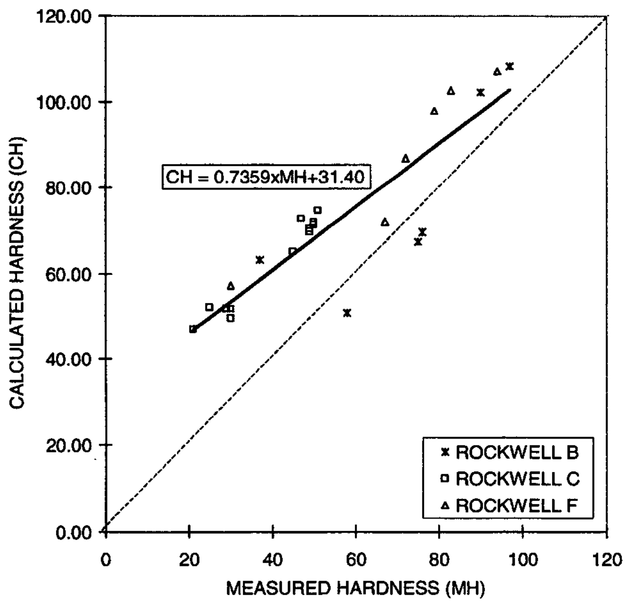

Figure 5. Plot of calculated Rockwell hardness versus measured Rockwell hardness.

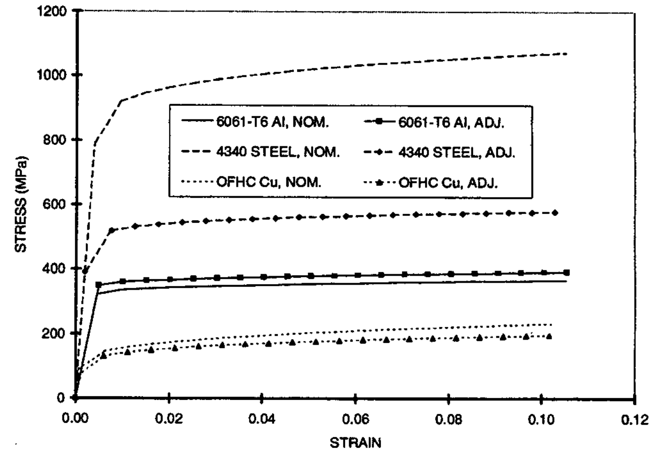

Figure 6. Comparison of nominal and adjusted stress-strain curves of three metals selected for a calculated hardness sensitivity study.

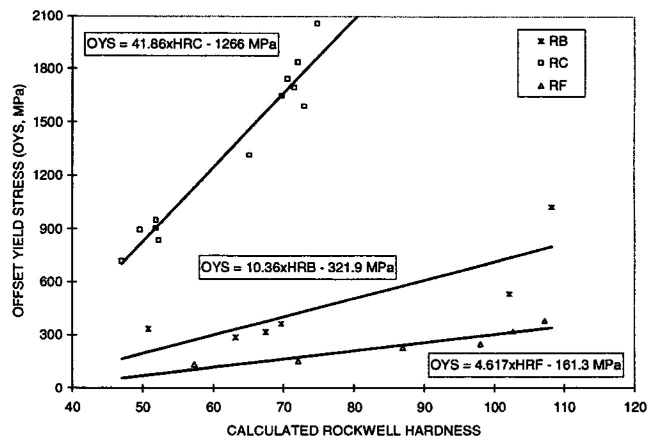

Figure 7. Plots of 0.2% offset yield stress (OYS) versus calculated Rockwell hardness number for a wide variety of different metals.